JOURNAL OF APPLIED ELECTROCHEMISTRY 24 (1994) 495–502

Current behaviour under periodic excitation during the anodic dissolution of copper

Z. H. GU, J. CHEN‡, T. Z. FAHIDY*

Department of Chemical Engineering, University of Waterloo, Ontario, Canada N2L 3G1

Received 10 May 1993; revised 1 December 1993

Current oscillations observed during the anodic dissolution of copper under sinusoidal and square wave potential perturbations are analysed via certain techniques of nonlinear dynamics. Low order Fourier expansions, and Poincaré maps indicate the existence of essentially nonchaotic characteristic structures.

List of symbols

a_k, A_k	Fourier cosine coefficient of the kth harmonic
b_k, B_k	Fourier sine coefficient of the kth harmonic
C_k	Fourier harmonic amplitude; $C_k = (A_k + B_k)^{1/2}$
f	frequency (s^{-1})
$G(j\omega)$	transfer function (or frequency spectrum)
i	current density ($mA\,cm^{-2}$)
j	imaginary parameter; $j = (-1)^{1/2}$
M	magnitude of a transfer function
T	period of an oscillation (s)
t	time (s)
V_a	anode potential (SCE)
$x(t)$	a function of time; x_0 its amplitude
Z_i	notation for the ith zone in Figs 2 and 7

Greek symbols

ϕ	short-hand for $\cos^2(2\pi t/T)$; Equation 6
ψ_k	phase angle associated with the kth harmonic
Ω	angular frequency of a sinusoidal forcing function ($rad\,s^{-1}$)
ω	angular frequency associated with the period of the null equation of the Duffing problem ($rad\,s^{-1}$)

1. Introduction

The anodic dissolution of copper into aqueous sodium chloride solutions containing small amounts of thyiocyanate ions under potentiostatic control has been the subject of an intensive investigation in recent years [1–4]. Under carefully controlled experimental conditions, a wide variety of oscillation patterns with high sensitivity to electrolyte composition, pH and anode potential, has been observed. The complex nature of oscillation patterns is most likely related to an insufficiently understood reaction/adsorption/desorption mechanism suggested by direct visualization of the anode surface and *in situ* morphological examinations [5].

The purpose of this paper is to analyse the oscillatory behaviour of anodic current due to periodic waves imposed on the *a priori* constant anode potential, in search for a better understanding of the nonlinear characteristics of oscillation. Analysis is carried out on experimental current–time series obtained under essentially unsteady-state conditions, given that the onset of oscillations is always found within a transient current response regime following the imposition of a constant anodic potential. In this respect, the approach is complementary to techniques perturbing a steady state of which the impedance technique has reached [6, 7] prominence in recent years. It can be used in the latter sense as well, when the complexity of the electrode process renders various impedances difficult to interpret.

2. Experimental details

Figure 1 illustrates the apparatus, whose details have been described previously [4]. The electrolytic cell contained a circular pure copper disc anode with a $50\,mm^2$ geometric area at the onset of current flow, and a pure copper plate cathode of a $1000\,mm^2$ active area, placed at a distance of 3.5 cm from the anode. The anode potential was set by a PAR 273 microcomputer-controlled potentiostat; sinusoidal and square wave modulation was provided by a Model 203A HP variable phase programmable function generator. The current–time series was recorded by the microcomputer at a sampling rate of 0.2 s. The electrolyte was an aqueous mixture of $4\,mol\,dm^{-3}$ NaCl and $1\,mmol\,dm^{-3}$ KSCN. The electrolyte had an initial pH of 6.7 and its temperature was kept between 19° C and 21° C. The range of the modulation frequency and amplitude was established in exploratory runs prior to the main set of experiments.

* Author to whom all correspondence should be addressed.
‡ Permanent address: The Research Institute of Shanghai Petrochemical Complex Shanghai 200540 PRC.

0021-891X

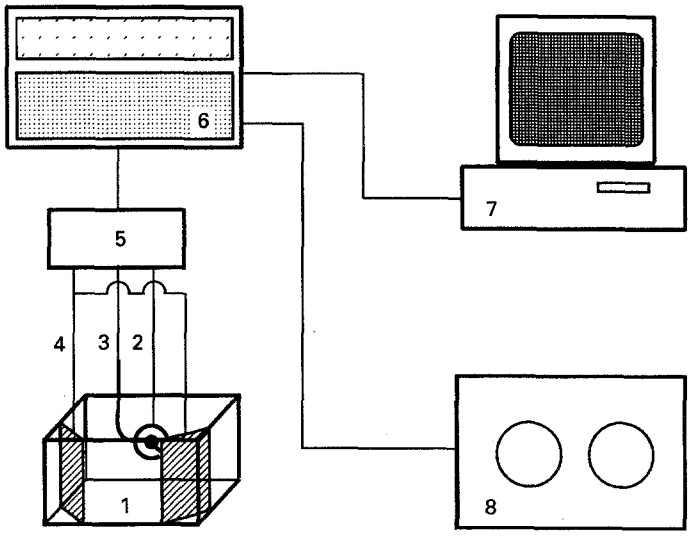

Fig. 1. Experimental apparatus: (1) cell; (2) working electrode; (3) reference electrode (saturated calomel); (4) counter electrode; (5) connector; (6) potentiostat/galvanostat; (7) microcomputer; (8) variable phase function generator.

3. Theoretical background and methods

Under a periodic perturbation, the response of a linear system possesses the same wave form as the perturbation and its amplitude and phase is determined by the system transfer function (also called the frequency spectrum). By contrast, the response of nonlinear systems to a periodic perturbation is highly specific, since nonlinear systems do not have transfer functions. The classical describing function technique [8, 9], which truncates the Fourier series of the oscillating output to the term carrying the fundamental input frequency, has been an important means of analysing closed-loop control system stability. In a general case, however, there is no guarantee that harmonic amplitudes will rapidly decrease in the Fourier series. In the case of certain power function nonlinearities the Fourier expansion becomes a simple polynomial in terms of the sine or cosine function. The output Fourier series may be regarded, therefore, as a 'fingerprint' of a nonlinear system subjected to a sinusoidal perturbation with a specific amplitude and frequency. A particularly interesting illustration is the classical Duffing problem of a single pendulum under periodic forcing [10] whose solution is extremely sensitive to parameters multiplying the linear and cubic term of the governing differential equation.

Periodic perturbations carrying several sinusoidal functions have also been proven useful in system analysis. As shown by Takahashi *et al.* [11], the response of a linear system to square wave perturbation with Fourier expansion

$$x(t) = x_0\left[\frac{1}{2}+\frac{2}{\pi}\sum_{m=1}^{\infty}\frac{\sin(m\omega_0 t)}{m}\right] \qquad \begin{cases} m = 2n+1 \\ n = 0, 1, \ldots \end{cases} \tag{1}$$

may be written as

$$y(t) = x_0\left[\frac{M_0}{2}+\frac{2}{\pi}\sum_{m=1}^{\infty}\frac{M_m\sin(m\omega_0 t+\phi_m)}{m}\right] \tag{2}$$

where $m_\mu|G(\mathrm{j}m\omega_0)|$; $\phi_m \equiv \arg G(\mathrm{j}m\omega_0)$ and $M_0 \equiv \lim|G(\mathrm{j}\omega)|$ as $\omega \longrightarrow 0$. It follows, in principle, that a single square wave perturbation of a preset frequency imposed on a linear system delivers its entire frequency response. In the case of nonlinear systems no such luxury exists and the response can be very complex. This is well illustrated by the output of a cubic nonlinearity subjected to an input of $x(t) = A_1 \sin\omega t + A_3 \sin 3\omega t$ [12]. Similarly, the classical approach of Lorenz to the dynamics of thermal convection [13] is based on the first three modes of the Fourier series of input perturbation. It is instructive to note that the distinction between single sinusoidal forcing and a harmonic series type forcing is somewhat arbitrary, due to the equivalence relationship [10], discussed briefly in the Appendix, which is a key element in treating the Duffing problem.

The ability of periodic perturbations in systems analysis is not confined to deterministic structures. The general Fourier series representation

$$F(t) = \frac{a_0}{2}+\sum_{k=1}^{\infty}(a_k\cos\omega_k t + b_k\sin\omega_k t) \tag{3}$$

also serves as basis for the establishment of the power spectrum of fluctuating outputs with Gaussian random characteristics [14]. The output power spectrum is simply the sum of the $(a_k^2 + b_k^2)$ terms divided by the length of the output interval, where a_k and b_k are coefficients of the Fourier series for the periodic function coinciding with the output function over this interval.

In recent years, alternative/complementary methods of nonlinear system analysis have been introduced with the advent of the modern theory of systems dynamics. In analysing system structures from experimentally obtained output functions with *a priori* unknown nonlinear characteristics regression methods [15], sequential pattern recognition [16] and heuristic techniques [17] exhibit various degrees of mathematical encumbrance and approximativeness. The graphical approach via phase portraits and Poincaré maps [11, 18–20] employs a sampled-data

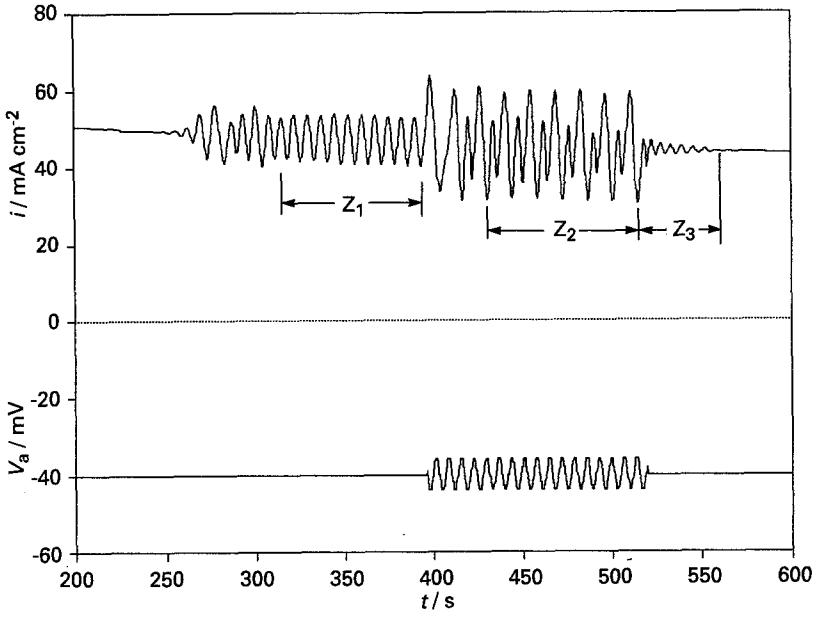

Fig. 2. Anode current oscillation patterns at constant potential and sinusoidal potential pulsing. $V_a = -40 \pm 4$ mV; $f = 0.14$ Hz.

sequence $Y_{n+1} = f(Y_n)$, where Y_n is an observation at sampling time t_n. With a driving 'motion' of period T, $t_n = nT + \tau_0$ is conventionally chosen such that τ_0 is an appropriate time delay. The collection of (Y_{n+1}, Y_n) points in a two-dimensional plane is the Poincaré map. Routinely used in the study of chaotic behaviour, this approach has been very useful in identifying periodic attractors in driven oscillators.

4. Analysis of the experimental observations

4.1. *Behaviour under sinusoidal-forcing*

A typical experimental observation, shown in Fig. 2, indicates the existence of three oscillatory zones. The onset of the first zone (Z_1) coincides with the full coverage of the anode surface by a mixture of Cu_2O and CuO (the oxide layers build up gradually while the anode potential is kept constant). In the absence of sinusoidal forcing zone Z_2 is not observed, hence zone Z_3 follows zone Z_1 immediately. Sinusoidal forcing creates a more complex oscillation structure; upon cessation of forcing, oscillation gradually vanishes (end of zone Z_3). Harmonic analysis of zone Z_2 yields the Fourier series approximation

$$i(t) \simeq 45.301 - 0.506\cos\frac{2\pi}{7}t - 7.441\cos\frac{4\pi}{7}t - 1.461\cos\frac{6\pi}{7}t \ldots \quad (4)$$

to the experimental time series, by neglecting terms with amplitudes less than unity in Table 1. The associated phase portrait in Fig. 3 indicates a consistently two-peak periodic behaviour. Similar observations in various anodic dissolution systems have also been described [21, 22]. Two-peak periodic behaviour can also be demonstrated theoretically for systems with Rössler dynamics [19, 23]. The sensitivity of the oscillation pattern to the frequency of forcing is demonstrated in Figs 4–6. The effect of the bias value of the anode potential was found to be negligible in the −40––50 mV (SCE) range. Similarly, the amplitude of the sinusoidal input function has a negligible effect on oscillation structure in the 4–8 mV range of the oscillation amplitude.

Table 1. Summary of the harmonic analysis associated with zone Z_2 in Fig. 2 fundamental period $T = 7$ s*

Harmonic number, K	A_k	B_k	C_k	ψ_k */degree*
0	90.60	–	90.60	–
1	0.51	2×10^{-5}	0.51	89.98
2	−7.44	5×10^{-5}	7.44	−90.41
3	−1.46	7×10^{-5}	1.46	−89.99
4	−0.63	9×10^{-5}	0.63	−89.17
5	−0.27	1×10^{-4}	0.27	−89.97
6	−0.08	1.4×10^{-4}	0.08	−89.90
7	−0.08	1.6×10^{-4}	0.08	−89.88
8	0.05	1.8×10^{-4}	0.05	89.79
9	$< 10^{-3}$	2.0×10^{-4}	0.001	88.84
10	0.04	2.3×10^{-4}	0.04	89.68

* The approximation is expressed as $\sum_k C_k \sin(2k\pi/T' + \psi_k)$.

4.2. *Behaviour under square-wave forcing*

As shown in Fig. 7, the oscillation structure is strongly nonlinear, and oscillation can persist in constant potential subperiods (zones Z_1 and Z_3) as in the case of sinusoidal forcing. Fourier analysis yields harmonics of irregularly varying amplitudes, consequently, Fourier series representation becomes uninviting. The associated phase portraits (Figs 8 and 9) demonstrate the deregularizing effect of square-wave forcing on the shape of the sinusoidal forcing-related attractor. The square wave-related attractor possesses its own characteristic shape. Sensitivity to the fundamental period of the square

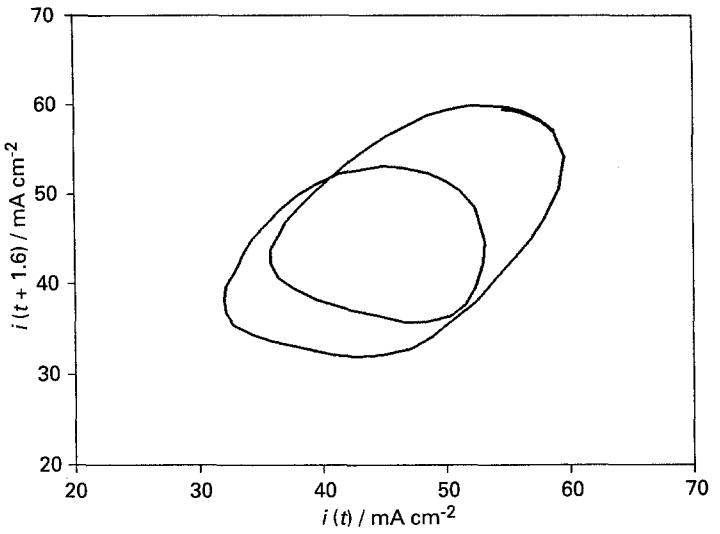

Fig. 3. Phase portrait/Poincaré map associated with Fig. 2, zone Z_2. $\tau_0 = 1.6$ s

wave is high as depicted in Figs 10 and 11; the resurgence of oscillation after a relatively quiescent time interval at low wave periods is an apparent 'fingerprint' of current response to square wave potential excitation; this phenomenon is not understood at present. The input amplitude effect is similar to that discussed in Section 4.1.

4.3. *Comparison with reference structures*

Two specific classes of experiments may be considered to constitute reference conditions. The first class consists of sinusoidal perturbation experiments with electrolytes containing no thiocyanate ions. As shown in Fig. 12, current oscillations are observed only in the oscillating potential regime, and they possess a highly regular, single period structure (the associated phase portrait is not shown). The absence of current oscillation at constant anode potentials was found to be independent of the numerical value of the potential.

The second reference class are experiments with constant anode potentials, when the electrolyte contains thiocyanate ions, e.g. zone Z_1 in Fig. 2. From Table 2, the oscillating anodic current density may be closely approximated by the truncated Fourier expansion

$$i \simeq 48.171 - 5.413\cos\frac{2\pi}{7}t - 0.288\cos\frac{4\pi}{7}t \ldots \quad (5)$$

so far as the harmonic terms for $k > 2$ possess amplitudes less than one tenth of C_2. The associated phase portrait (omitted) is a highly regular ellipse in the $i(t+1.6)/i(t)$ plane.

Table 2. Summary of the harmonic analysis associated with zone Z_1 in Fig. 2 fundamental period $T = 7$ s*

Harmonic number, K	A_k	B_k	C_k	ψ_k */degree*
0	96.34	–	96.34	–
1	−5.413	5×10^{-5}	5.413	−90.00
2	−0.288	1.1×10^{-5}	0.288	−89.98
3	−0.029	1.6×10^{-4}	0.029	−89.68
4	−0.029	2.1×10^{-4}	0.029	−89.57

* The approximation is expressed as $\sum_k C_k \sin(2k\pi t/T + \psi_k)$; for $k > 4$, $|C_k| \leq 0.01$.

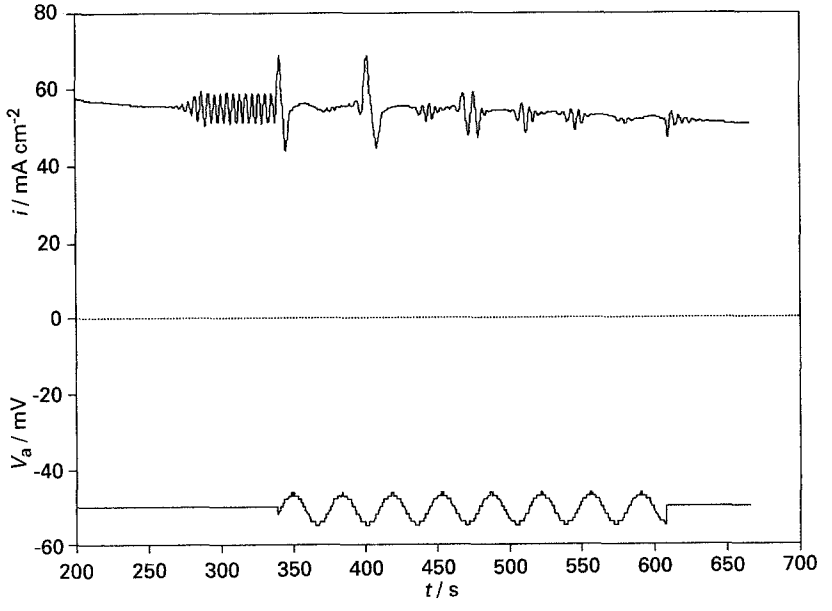

Fig. 4. Anode current oscillation patterns at constant potential and sinusoidal potential pulsing. $V_a = -50 \pm 4$ mV; $f = 0.0285$ Hz.

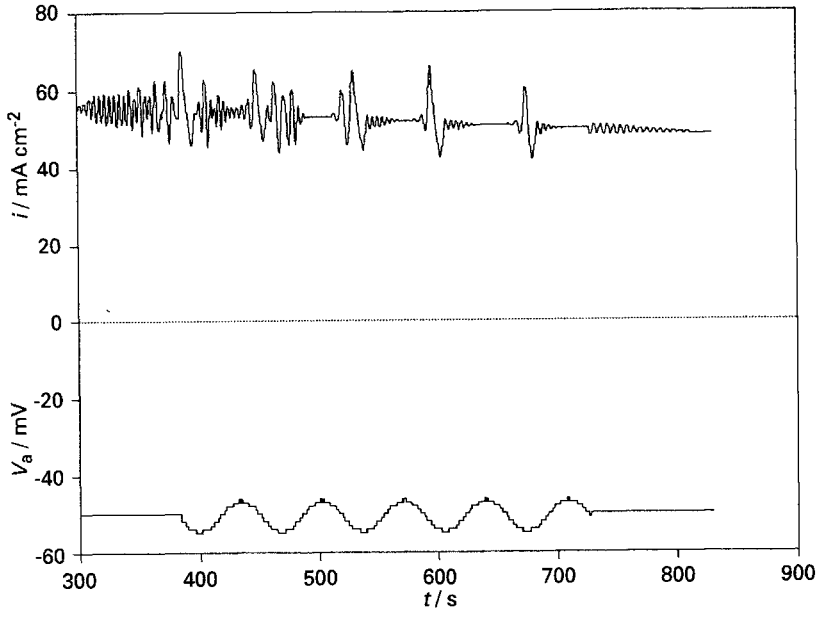

Fig. 5. Anode current oscillation patterns at constant potential and sinusoidal potential pulsing. $-V_a = -50 \pm 4\,\text{mV}$; $f = 0.015\,\text{Hz}$.

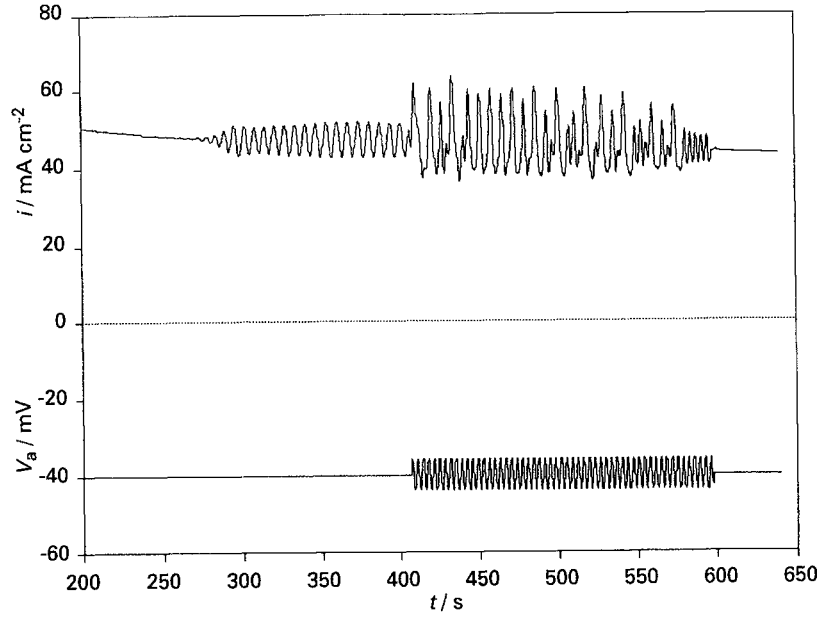

Fig. 6. Anode current oscillation patterns at constant potential and sinusoidal potential pulsing. $V_a = -40 \pm 4\,\text{mV}$; $f = 0.285\,\text{Hz}$.

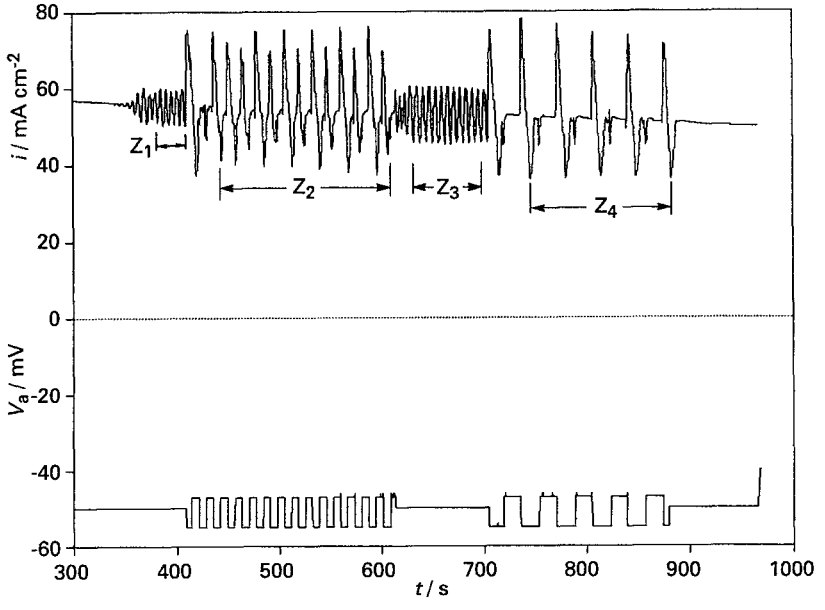

Fig. 7. Anode current oscillation patterns at constant potential and square wave potential pulsing. $V_a = -40 \pm 4\,\text{mV}$; $f = 0.071$ and $0.0285\,\text{Hz}$.

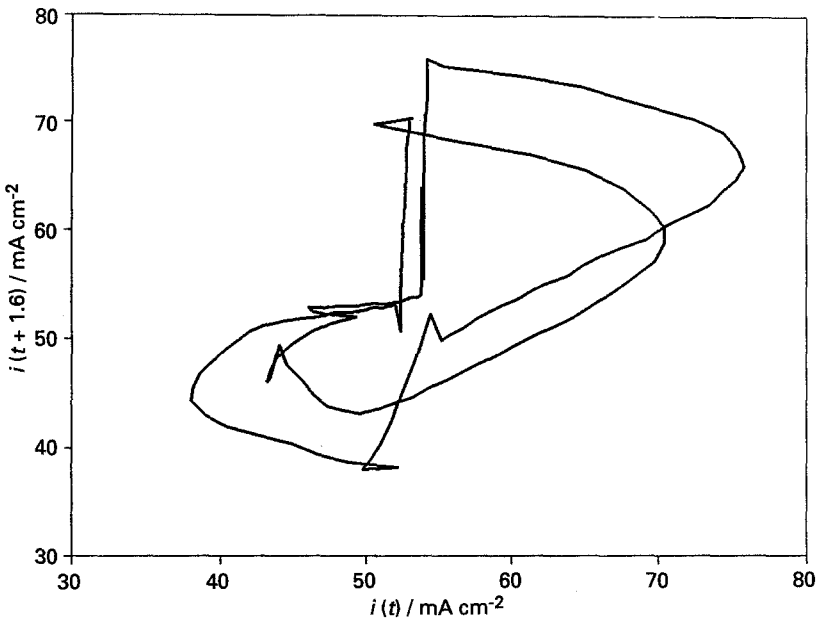

Fig 8. Phase portrait/Poincaré map associated with Fig. 7, zone Z_2. $\tau_0 = 1.6$ s.

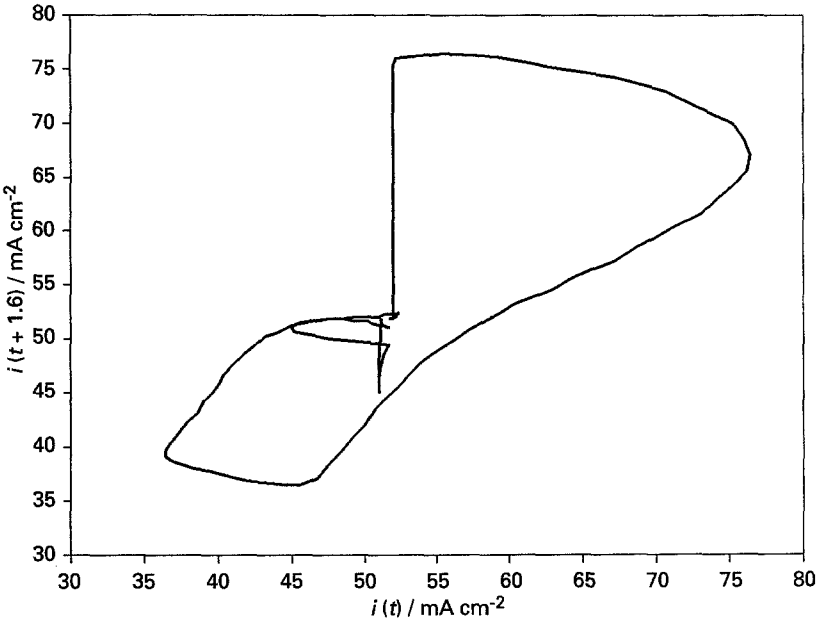

Fig. 9. Phase portrait/Poincaré map associated with Fig. 7, zone Z_4. $\tau_0 = 1.6$ s.

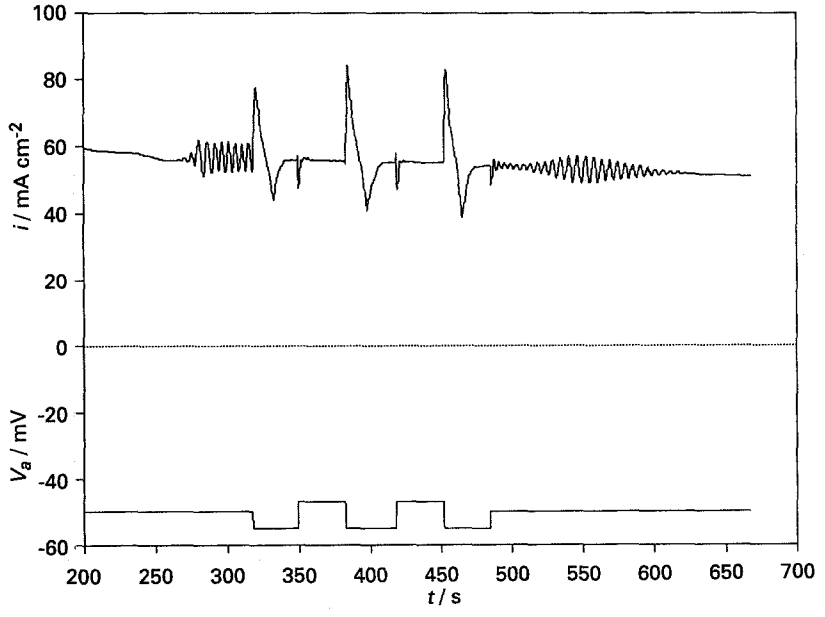

Fig. 10. Anode current oscillation patterns at constant potential and square wave potential pulsing. $V_a = -50 \pm 4$ mV; $f = 0.015$ Hz.

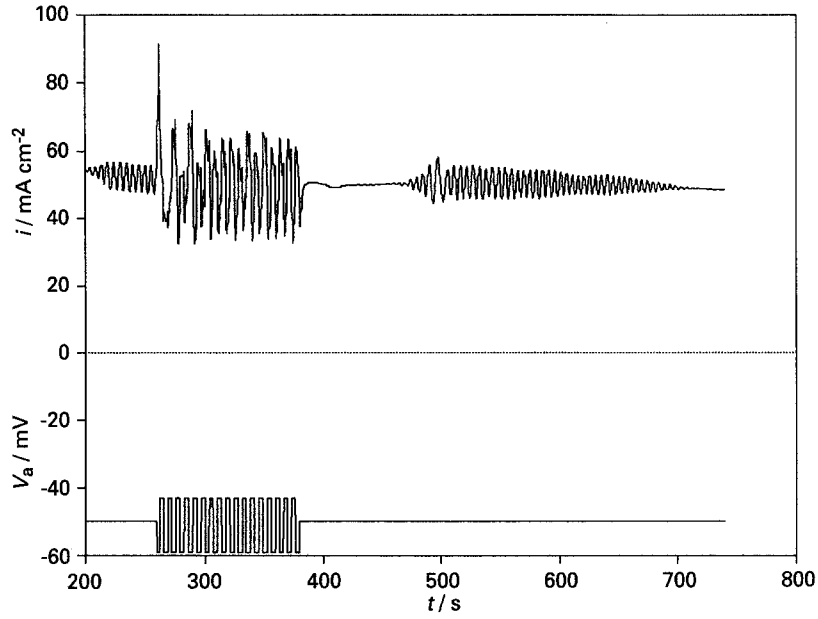

Fig. 11. Anode current oscillation patterns at constant potential and square wave potential pulsing. $V_a = -50 \pm 4$ mV; $f = 0.071$ Hz.

5. Discussion

The oscillatory nature of anodic copper dissolution is determined by a complex reaction mechanism involving the CuCl, Cu_2O, CuO and CuSCN species [3–5, 24]. In the tentatively proposed qualitative adaptation [3] of the Brusselator model of chemical reactions [25] the onset of oscillation at a constant anode potential was related to a Hopf bifurcation involving the rate of cuprous ion and cuprous chloride kinetics. The employment of sinusoidal anode potential inputs permits an alternative mathematical interpretation in terms of the apparent mathematical characteristics associated with the electrode surface. It follows from Fourier analysis of data assembled in Tables 1 and 2 that the current response to excitation via both constant *and* sinusoidal potentials may be expressed as

$$i \simeq \sum_{k=0}^{N} \beta_k \phi^k; \quad \phi \equiv \cos^2 \frac{\pi t}{T} \tag{6}$$

where β_k are experimentally determined coefficients, on account of (elementary) relationships between powers of the cosine function of an angle, and cosines of its multiples.

Specifically, in zone Z_1

$$i \simeq 53.291 - 8.5\phi - 2.32\phi^2 \tag{7a}$$

and in zone Z_2

$$i \simeq 38.811 + 34.26\phi + 10.56\phi^2 - 46.72\phi^3 \tag{7b}$$

Thus, excitation via a constant anode potential generates a purely circular limit cycle reminiscent of the Duffing system with sufficiently small input amplitudes in a system with cubic nonlinearity [26], or of a Van der Pol system with a sufficiently small coefficient ϵ of the nonlinear term of the classical Van der Pol equation in nonlinear mechanics [27]. The negative term in Equation 7(b) precludes the assumption of a single exponential nonlinearity of the form V^n; n an integer, but a polynomial type nonlinearity similar to the Duffing system [10], or a structure of the Van der Pol equation with high ϵ-coefficients may well serve as analogoues (a quantitative identification via

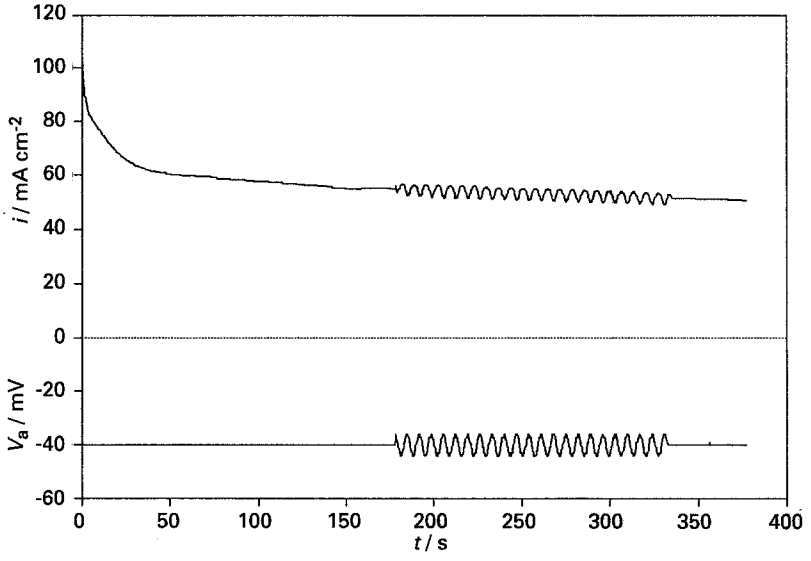

Fig. 12. A typical oscillation pattern observed in the absence of thiocyanate ions. $V_a = -40 \pm 4$ mV; $f = 0.15$ Hz.

nonlinear oscillator theory is beyond the scope of this paper).

As stated in Section 4.2, current oscillations due to square wave anode potential excitation are not amenable to Fourier analysis. The phase portraits shown in Figs 8 and 9 indicate the essentially limit-cycle nature of the current oscillations (with one or more periods). A slight tendency to irregularity is indicated by non-monotonic sectors of the trajectories; however, no strange attractor can be specifically identified.

6. Conclusions

The new experimental data and their analysis presented in this paper provide further evidence for the essentially nonchaotic oscillatory behaviour caused by thiocyanate ions. The structure of oscillations appears to be (at least qualitatively) similar to two classical nonlinear oscillators. While current understanding of the reaction mechanisms, which determine the overall anodic dissolution, is rather limited, future studies of oscillations coupled with *in situ* surface-scanning analyses should facilitate a quantitative determination of kinetic parameters. The approach applied to anodic copper dissolution into aqueous NaCl/KSCN solutions may readily be extended to the anodic dissolution of various substances, which involve oscillating currents.

Acknowledgement

This and similar research has been supported by the Natural Sciences and Engineering Research Council of Canada (NSERC).

References

[1] Z. H. Gu and T. Z. Fahidy, *Can. J. Chem. Eng.* **70** (1992) 127.
[2] Z. H. Gu, A. Olivier and T. Z. Fahidy, *Electrochim. Acta* **35** (1990) 933.
[3] Z. H. Gu, J. Chen and T. Z. Fahidy, *ibid*, **37** (1992) 2637.
[4] Z. H. Gu, J. Chen, A. Olivier and T. Z. Fahidy, *J.* Electrochem. Soc. **140** (1993) 108.
[5] Z. H. Gu, J. Chen and T. Z. Fahidy, 'The effect of process parameters on the anodic dissolution of copper into NaCl/KSCN electrolytes', *J. Electroanal. Chem.*, in press.
[6] A. J. Bard and L. R. Faulkner, 'Electrochemical Methods', Wiley, New York (1980) Chapter 9.
[7] C. Gabrielli, 'Identification of electrochemical processes by frequency response analysis', Technical Report 004/83 CNRS GR4 Phys. des Liquides et Electrochimie, Université P. et M. Curie, Paris (1984).
[8] J. C. West, 'Analytical Techniques for Non-Linear Control Systems', Van Nostrand, New York (1960) Chapters 9–11.
[9] D. Graham and D. McRuer, 'Analysis of Nonlinear Control Systems', Dover, New York (1971) Chapters 3, 4 and 6.
[10] H. T. Davis, 'Introduction to Nonlinear Differential and Integral Equations', US Government Printing Office, Washington, DC (1961) Section 12.8.
[11] Y. Takahashi, M.J. Rabins and D.M. Auslander, 'Control and Dynamic Systems', Addison-Wesley, Reading, MA (1970) Section 9.4.
[12] J. C. West, *op. cit.* [8] Section 10.2.
[13] J. M. T. Thompson and H. B. Stewart, 'Nonlinear Dynamics and Chaos', Wiley, New York (1986) Section 11.1.
[14] V. V. Solodovnikov, 'Introduction to the Statistical Dynamics of Automatic Control Systems', Dover, New York (1960) Section 7.
[15] D. Graupe, 'Identification of Systems', Van Nostrand Reinhold, New York (1972) Section 5.6.
[16] *Idem, ibid*, Section 7.3.
[17] *Idem, ibid*, Chapter 11.
[18] F. C. Moon, 'Chaotic Vibrations', Wiley, New York (1987) Chapter 2.
[19] P. G. Drazin, 'Nonlinear Systems', Cambridge University Press, Cambridge, GB (1992) Chapters 6–8.
[20] K. Tomita, 'Periodically Forced Nonlinear Oscillators' *in* 'Chaos' (edited by A. V. Holden), Princeton University Press, Princeton NJ (1986) Chapter 10.
[21] M. R. Bassett and J. L. Hudson, *J. Electrochem. Soc.* **137** (1990) 922.
[22] *Idem, ibid.* **137** (1990) 1815.
[23] O. E. Rössler, *Phys. Lett.* **A57** (1976) 397.
[24] Z. H. Gu, T. Z. Fahidy and J. P. Chopart, *Electrochim. Acta* **37** (1992) 97.
[25] J. M. T. Thompson and H. B. Stewart, *op. cit.* [13], Section 4.3.
[26] D. Graham and D. McRuer, *op cit.* [9], Section 5.2.
[27] H. T. Davis, *op. cit.* [10], Section 12.2.

Appendix: A brief discussion of the duffing problem [10]

The trajectory of a simple pendulum moved by a sinusoidal driving force is given by integrating the nonlinear equation [10]

$$\frac{d^2y}{dt^2} + y + ry^3 = K \sin \Omega t \qquad (A.1)$$

where r is a real parameter. If the solution is sought in terms of a Fourier series

$$y = \sum_{k=1}^{\infty} a_{2k+1} \sin(2k+1)\omega t \qquad (A.2)$$

where ω is the frequency of the null-equation associated with $K = 0$ in Equation A.1, then it is advantageous to replace the driving force by a harmonic representation

$$K \sin \Omega t = \sum_{j=1}^{\infty} K_{2j+1} \sin(2j+1)\omega t$$

$$K_{2j+1} = \frac{2}{\pi} \frac{K \sin \mu}{\mu^2 - (2j+1)^2}; \quad \mu \equiv \Omega/\omega \qquad (A.3)$$

The time series form of the solution and associated phase trajectories (dy/dt plotted against y) are sensitive to the parameters in Equation (A.1); a typical case where $r = -1/6$, $K = 2$ and $\mu = 3$ is discussed in detail by Davis [10, pp. 390–4], as well as the more difficult case of $\mu \simeq 1$ (nonlinear resonance).

The equivalence relationship in Equation A.3 implies the usefulness of perturbation functions expressible via Fourier series, e.g. the square wave function employed in this work, in the study of dynamic behaviour. Deviations from response to a single sinusoidal perturbation serves as a measure of nonlinearity, especially in terms of the specific characteristics of phase portraits.